

Ascertaining the influences of auxiliary qubits on the Einstein-Podolsky-Rosen steering and its directions

Ling-Ling Xing(邢玲玲), Huan Yang(杨欢), Gang Zhang(张刚) and Min Kong(孔敏)

Citation: Chin. Phys. B, 2024, 33 (**5**): 050304. DOI: 10.1088/1674-1056/ad1927
Journal homepage: http://cpb.iphy.ac.cn; http://iopscience.iop.org/cpb

What follows is a list of articles you may be interested in

Genuine Einstein-Podolsky-Rosen steering of generalized three-qubit states via unsharp measurements

Yuyu Chen(陈玉玉), Fenzhuo Guo(郭奋卓), Shihui Wei(魏士慧), and Qiaoyan Wen(温巧燕)
Chin. Phys. B, 2023, 32 (**4**): 040309. DOI: 10.1088/1674-1056/acac14

High-fidelity universal quantum gates for hybrid systems via the practical photon scattering

Jun-Wen Luo(罗竣文) and Guan-Yu Wang(王冠玉)
Chin. Phys. B, 2023, 32 (**3**): 030303. DOI: 10.1088/1674-1056/ac8734

Deterministic remote state preparation of arbitrary three-qubit state through noisy cluster-GHZ channel

Zhihang Xu(许智航), Yuzhen Wei(魏玉震), Cong Jiang(江聪), and Min Jiang(姜敏)
Chin. Phys. B, 2022, 31 (**4**): 040304. DOI: 10.1088/1674-1056/ac2b17

Generation of tripartite Einstein-Podolsky-Rosen steering by cascaded nonlinear process

Yu Liu(刘瑜), Su-Ling Liang(梁素玲), Guang-Ri Jin(金光日), You-Bin Yu(俞友宾), Jian-Yu Lan(蓝建宇), Xiao-Bin He(何小斌), Kang-Xian Guo(郭康贤)
Chin. Phys. B, 2020, 29 (**5**): 050301. DOI: 10.1088/1674-1056/ab7da6

Efficient scheme for remote preparation of arbitrary *n*-qubit equatorial states

Xin-Wei Zha(查新未), Min-Rui Wang(王敏锐), Ruo-Xu Jiang(姜若虚)
Chin. Phys. B, 2020, 29 (**4**): 040304. DOI: 10.1088/1674-1056/ab773d

---

Ascertaining the influences of auxiliary qubits on the Einstein–Podolsky–Rosen steering and its directions

Ling-Ling Xing(邢玲玲), Huan Yang(杨欢)†, Gang Zhang(张刚)‡, and Min Kong(孔敏)

School of Electrical and Photoelectronic Engineering, West Anhui University, Lu'an 237012, *China*

(Received 7 November 2023; revised manuscript received 27 December 2023; accepted manuscript online 28 December 2023)

Einstein–Podolsky–Rosen (EPR) steering is an example of nontrivial quantum nonlocality and characteristic in the non-classical world. The directivity (or asymmetry) is a fascinating trait of EPR steering, and it is different from other quantum nonlocalities. Here, we consider the strategy in which two atoms compose a two-qubit X state, and the two atoms are owned by Alice and Bob, respectively. The atom of Alice suffers from a reservoir, and the atom of Bob couples with a bit flip channel. The influences of auxiliary qubits on EPR steering and its directions are revealed by means of the entropy uncertainty relation. The results indicate that EPR steering declines with growing time t when adding fewer auxiliary qubits. The EPR steering behaves as damped oscillation when introducing more auxiliary qubits in the strong coupling regime. In the weak coupling regime, the EPR steering monotonously decreases as t increases when coupling auxiliary qubits. The increases in auxiliary qubits are responsible for the fact that the steerability from Alice to Bob (or from Bob to Alice) can be more effectively revealed. Notably, the introductions of more auxiliary qubits can change the situation that steerability from Alice to Bob is certain to a situation in which steerability from Bob to Alice is certain.

Keywords: auxiliary qubits, EPR steering, directions, influence

PACS: 03.67.–a, 03.65.Yz, 03.65.Ud **DOI:** 10.1088/1674-1056/ad1927

1. Introduction

Over the years, more and more non-classical phenomena have been revealed by investigating the quantum world. Revelation of these non-classical phenomena has led to a deep understanding of different quantum nonlocalities. Among them is a phenomenon called spooky-action-at-distance.[1,2] That is, if two entangled particles are possessed by Alice and Bob, respectively, then Alice can immediately steer the particle of Bob by executing a measurement on her particle. This fascinating phenomenon is believed to be the origin of studying Einstein–Podolsky–Rosen (EPR) steering (or quantum steering).[3] Subsequently, EPR steering was formally and rigorously defined from quantum information tasks.[4] This outstanding contribution is regarded as the beginning of theoretical and experimental explorations of EPR steering.[3] Relevant investigations involve the detection of EPR steering, the concept of EPR steering, joint measurability and EPR steering, the application of EPR steering, and so on.[3] The detection of EPR steering is an important topic and hotspot in the field of EPR steering. One can use various steering criteria to capture EPR steering, such as the full information steering criterion,[5] linear and nonlinear steering criteria,[6,7] a steering criterion based on a geometric Bell-like inequality[8,9] and steering criteria of uncertainty relations.[10–16] Based on the detection of EPR steering, EPR steering has been used to ascertain subchannel discrimination, temporal and channel steering, randomness certification, secret sharing and quantum key distribution.[3]

Recently, examinations of EPR steering in different systems have been conducive to the practical application of EPR steering, and investigations have also helped to recognize the nonclassical traits of various systems, including non-Markovian systems,[17] non-Gaussian spin systems,[18] atom systems,[19] neutrino oscillations[20] and quantum dot systems.[21] In general, experimental realizations are important for theoretical applications in quantum information. For this purpose, relevant explorations of EPR steering have been implemented using various experimental settings.[22–28] For instance, in the optical non-Gaussian state, the relationship between remotely created Wigner negativity and EPR steering was demonstrated by Liu *et al.*[22] Wollmann *et al.* explored the robustness of EPR steering in optical systems.[14] Considering an optical setting, Yang *et al.* experimentally realized the observation of EPR steering via entanglement detection,[26] predicted EPR steering via quantum entanglement[27] and also demonstrated complementarity relations between the EPR steering criteria of optical systems.[28] These efforts have deepened our understanding of EPR steering and its applications in both theory and experiment. Of particular note is that a unique characteristic of EPR steering is asymmetry (or directivity),[3] including one-way EPR steering and two-way EPR steering.[3] However, the investigations mentioned above did not involve the asymmetry (or directivity) of EPR steering.

Fortunately, due to the nontrivial application of the asymmetry of EPR steering in one-sided device-independent

†Corresponding author. E-mail: hyang@wxc.edu.cn

‡Corresponding author. E-mail: zhanggang@wxc.edu.cn

© 2024 Chinese Physical Society and IOP Publishing Ltd

quantum key distribution,[3] observations of the asymmetry of EPR steering have been gradually implemented in different systems. For instance, optical systems,[29] self-phase-locked optical parametric oscillators,[30] dynamical Casimir arrays,[31] high dimension systems,[32] modulated optomechanical systems,[33] cavity magnonics,[34] macroscopic hybrid systems,[35] and so on. Reservoir systems are an important physical model, and the maximal-steered-coherence of such systems can be controlled by quantum reservoir engineering.[36] In addition, maximal-steered-coherence can be converted to quantum entanglement through optimal incoherent operation and incoherent ancilla in reservoir systems;[37] the results reveal the importance of active quantum operations on the control of quantum nonlocalities in reservoir systems. However, the influence of auxiliary qubits on EPR steering and its directions in reservoir system is unknown, and relevant investigations are still lacking.

Motivated by this, we consider the situation in which two atoms compose a two-qubit X state, one of atoms couples with a reservoir and the other one suffers from a bit flip channel. We reveal the influence of auxiliary qubits on EPR steering and its directions by using the entropy uncertainty relation. The results indicate that EPR steering declines (it behaves as damped oscillation) with increasing time t if one introduces fewer (more) auxiliary qubits in the strong coupling regime. In the weak coupling regime, EPR steering monotonously decreases as t increases when coupling auxiliary qubits. The increase in auxiliary qubits is responsible for the fact that steerability from Alice to Bob (or from Bob to Alice) can be more effectively captured. Furthermore, the introduction of more auxiliary qubits can change the direction of EPR steering which can be detected through the entropy uncertainty relation.

The structure of the paper is as follows. Section 2 briefly describes the theoretical model. Section 3 characterizes the EPR steering of a system via the entropy uncertainty relation. Under different parameters, the influences of auxiliary qubits on EPR steering and its directions are uncovered in Sections 4–6. Finally, Section 7 summarizes some conclusions that are drawn in this paper.

2. Theoretical model

We consider a model in which a common zero-temperature reservoir independently influences a system of N identical qubits (two-level atoms), and the N identical qubits decouple each other. The total Hamiltonian is ($\hbar = 1$)[36]

$$H = \sum_{j=1}^{N} \Xi_0 \sigma_j^+ \sigma_j^- + \sum_k \omega_k c_k^\dagger c_k + \sum_{j=1}^{N} \sum_k \left(\beta_k^j \sigma_j^+ c_k + \beta_k^{j*} \sigma_j^- c_k^\dagger \right). \tag{1}$$

For the j-th qubit, the lowering operator is $\sigma_j^- = (\sigma_j^+)^\dagger = |0\rangle\langle j|$ and Ξ_0 is the transition frequency between the ground state and the excited state. β_k^j is the coupling strength between the j-th atom and the k-th field mode. The k-th field mode has frequency ω_k and c_k ($c_k^\dagger$) is the annihilation (creation) operator of k-th field mode. Assuming $\beta_k^j = G_k/\sqrt{N}$, an alternative set of orthogonal basis can be defined by

$$|\varphi_l\rangle = \frac{1}{\sqrt{N}} \sum_{m=0}^{N-1} \exp\left(\frac{2\mathrm{i}\pi ml}{N}\right) |m+1\rangle, \quad (l = 0, 1, \ldots, N-1). \tag{2}$$

The total Hamiltonian is[36]

$$H = \sum_{j=0}^{N-1} \Xi_0 |\varphi_j\rangle\langle\varphi_j| + \sum_k \omega_k c_k^\dagger c_k + \sum_k \left(G_k |\varphi_0\rangle\langle 0| c_k + G_k^* |0\rangle\langle\varphi_0| c_k^\dagger \right). \tag{3}$$

This Hamiltonian means that the coupling between the reservoir and the system only includes the two-dimensional subspace of the eigenstate $|\varphi_0\rangle$ and the ground state $|0\rangle$. Thus, the other $N-1$ eigenstates ($|\varphi_1\rangle, |\varphi_2\rangle, \ldots, |\varphi_{N-1}\rangle$) do not suffer from the reservoir. Considering a system of N two-level atoms, the initial state of the system is

$$|\psi(0)\rangle = c_0(0)|0\rangle_{\mathrm{S}}|0\rangle_{\mathrm{E}} + \sum_{j=0}^{N-1} E_j(0)|\varphi_j\rangle_{\mathrm{S}}|0\rangle_{\mathrm{E}}. \tag{4}$$

$|0\rangle_{\mathrm{E}}$ ($|0\rangle_{\mathrm{S}}$) is the vacuum state of the field (the ground state of the system). The time-evolved state is[36]

$$|\psi(t)\rangle = c_0(t)|0\rangle_{\mathrm{S}}|0\rangle_{\mathrm{E}} + \sum_{j=0}^{N-1} E_j(t)|\varphi_j\rangle_{\mathrm{S}}|0\rangle_{\mathrm{E}} + \sum_k F_k(t)|0\rangle_{\mathrm{S}}|1_k\rangle_{\mathrm{E}}. \tag{5}$$

$|1_k\rangle_{\mathrm{E}}$ is the state of the reservoir with single excitation in the k-th field mode. $F_k(t)$ and $E_j(t)$ are time-dependent coefficients.

$$\frac{\mathrm{d}E_0(t)}{\mathrm{d}t} = -\mathrm{i}\Xi_0 E_0(t) - \mathrm{i}\sum_k G_k F_k(t), \tag{6}$$

$$\frac{\mathrm{d}F_k(t)}{\mathrm{d}t} = -\mathrm{i}\omega_k F_k(t) - \mathrm{i}G_k^* E_0(t). \tag{7}$$

The remaining coefficients are controlled by $\mathrm{d}E_j(t)/\mathrm{d}t = -\mathrm{i}\Xi_0 E_j$. The new coefficients $\tilde{E}_j(t) = \mathrm{e}^{\mathrm{i}\Xi_0 t} E_j(t)$ and $\tilde{F}_k(t) = \mathrm{e}^{\mathrm{i}\omega_k t} F_k(t)$ are introduced, and

$$\frac{\mathrm{d}\tilde{E}_0(t)}{\mathrm{d}t} = -\mathrm{i}\sum_k G_k \mathrm{e}^{\mathrm{i}(\Xi_0-\omega_k)t} \tilde{F}_k(t), \tag{8}$$

$$\frac{\mathrm{d}\tilde{F}_k(t)}{\mathrm{d}t} = -\mathrm{i}G_k^* \mathrm{e}^{-\mathrm{i}(\Xi_0-\omega_k)t} \tilde{E}_0(t). \tag{9}$$

Here, $\tilde{E}_j(t) = \tilde{E}_j(0)$. Integrating Eq. (9) and substituting it into Eq. (8), one can obtain[36]

$$\frac{\mathrm{d}\tilde{E}_0(t)}{\mathrm{d}t} = -\int_0^t f(t-t')\tilde{E}_0(t')\,\mathrm{d}t', \tag{10}$$

with

$$f(t-t') = \int_{-\infty}^{\infty} \mathrm{d}\omega\, \aleph(\omega)\, \mathrm{e}^{\mathrm{i}(\Xi_0-\omega)(t-t')}. \tag{11}$$

The $\aleph(\omega)$ represents the spectral density of the reservoir

$$\begin{aligned}\aleph(\omega) &= \sum_k |G_k|^2 \delta(\omega-\omega_k) \\ &= N\sum_k |\beta_k|^2 \delta(\omega-\omega_k) = NJ(\omega).\end{aligned} \tag{12}$$

Here, we consider

$$J(\omega) = \frac{1}{2\pi} \frac{\gamma_0 \lambda^2}{(\omega-\omega_\mathrm{c})^2+\lambda^2} \tag{13}$$

and this is the Lorentzian spectral density of the reservoir (the central frequency of the reservoir is represented by ω_c, the spectral width is represented by λ and the coupling strength is represented by γ_0). Assuming $\omega_\mathrm{c} = \Xi_0$, that is to say the qubits are in the exact resonance condition with the cavity field, the exact solution of $E_0(t)$ is[36]

$$\tilde{E}_0(t) = \mathrm{e}^{-\lambda t/2}\left[\cosh\left(\frac{Ft}{2}\right) + \frac{\lambda}{F}\sinh\left(\frac{Ft}{2}\right)\right]\tilde{E}_0(0), \tag{14}$$

with $F = \sqrt{\lambda^2 - 2N\gamma_0\lambda}$. $|\psi(t)\rangle$ in Eq. (5) is rewritten as[36]

$$\begin{aligned}|\psi(t)\rangle &= c_0(t)|0\rangle_\mathrm{S}|0\rangle_\mathrm{E} + \sum_{j=0}^{N-1} \Im_j(t)|j+1\rangle_\mathrm{S}|0\rangle_\mathrm{E} \\ &\quad + \sum_k F_k(t)|0\rangle_\mathrm{S}|1_k\rangle_\mathrm{E},\end{aligned} \tag{15}$$

with

$$\Im_j(t) = \frac{1}{\sqrt{N}} \sum_{m=0}^{N-1} \exp\left(\frac{2\mathrm{i}\pi m j}{N}\right) E_m(t). \tag{16}$$

Alice (A) and Bob (B) share two qubits (two-level atoms). The atom of Alice (the atom of Bob) couples with the local environment (is not subjected to the reservoir). Besides, some atoms are introduced to the common reservoir, and they couple with the reservoir. We assume that the first atom ($j=1$) (it can be excited) belongs to the system of Alice and the remaining atoms (in their ground states) belong to the auxiliary qubits.[36] If the initial probability amplitudes $\Im_1(0) = \Im_2(0) = \cdots = \Im_{N-1}(0) = 0$, the dynamic of probability amplitude is $\Im_0(t) = \wp(t)\Im_0(0)$ with[36]

$$\begin{aligned}\wp(t) &= \mathrm{e}^{-\mathrm{i}\Xi_0 t}\left\{\frac{N-1}{N}\right. \\ &\quad \left. + \frac{\mathrm{e}^{-\lambda t/2}}{N}\left(\cosh\left(\frac{Ft}{2}\right) + \frac{\lambda}{F}\sinh\left(\frac{Ft}{2}\right)\right)\right\}.\end{aligned} \tag{17}$$

The single state of Alice is[36]

$$\rho^\mathrm{A}(t) = \begin{pmatrix} \rho_{00}^\mathrm{A}(0) + \rho_{11}^\mathrm{A}(0)(1-p(t)) & \rho_{01}^\mathrm{A}(0)\sqrt{p(t)} \\ \rho_{10}^\mathrm{A}(0)\sqrt{p(t)} & \rho_{11}^\mathrm{A}(0)p(t) \end{pmatrix}, \tag{18}$$

with $p(t) = |\wp(t)|^2$.

3. Characterizing EPR steering using the entropy uncertainty relation

More specifically, we consider the following scheme. A two-qubit X state

$$\rho_\mathrm{AB}^\mathrm{X} = \frac{1}{4}\left(I\otimes I + \boldsymbol{v}\cdot\boldsymbol{\sigma}\otimes I + I\otimes \boldsymbol{w}\cdot\boldsymbol{\sigma} + \sum_{i=1}^{3} t_i \sigma_i\otimes\sigma_i\right) \tag{19}$$

belongs to Alice (A) and Bob (B). $\boldsymbol{\sigma} = (\sigma_1, \sigma_2, \sigma_3)$ is the vector of the Pauli matrix, I is an identity operator, $\boldsymbol{v} = (0,0,v)$ and $\boldsymbol{w} = (0,0,w)$ are Bloch vectors. $t_i = \mathrm{Tr}(\rho_\mathrm{AB}^\mathrm{X}\sigma_i\otimes\sigma_i)$ $(i=1,2,3)$ is the matrix element of the spin correlation matrix. Considering a bit flip channel,[38] and the Kraus operators are

$$K_0(t) = \begin{pmatrix} \sqrt{k} & 0 \\ 0 & \sqrt{k} \end{pmatrix}, \quad K_1(t) = \begin{pmatrix} 0 & \sqrt{1-k} \\ \sqrt{1-k} & 0 \end{pmatrix}. \tag{20}$$

This channel directly influences the atom of Bob $\rho_\mathrm{AB}^\mathrm{X}$, and does not affect the atom of Alice. Coupling between the atom of Bob and the bit flip channel can lead to the information stored in the system flowing from the system to the environment; thus it causes dissipation of the EPR steering of the system. That is, the physical motivation for the coupling between the atom of Bob and the bit flip channel is to accelerate the degeneration of EPR steering. The atom of Alice directly interacts with the reservoir mentioned above (together with $N-1$ auxiliary atoms). Namely, if there are N atoms, one is sent to Alice while the remaining atoms ($N-1$ atoms) are treated as auxiliary qubits. $N=1$ corresponds to the absence of auxiliary atom. The physical motivation of the interaction between the atom of Alice and the $N-1$ auxiliary atoms is that auxiliary atoms can influence the flow of information between the system and the reservoir, and give rise to the backflow of information from the reservoir to the system. This scenario can lead to an increase in the EPR steering and also help us to effectively reveal and protect the EPR steering. The final state is ρ_F, and the nonzero matrix elements of final state are

$$\begin{aligned}\rho_{\mathrm{F}11} &= \frac{1}{4}\{2 + w(4k-2) \\ &\quad + p[v+w-1-2kw+t_3(2k-1)]\},\end{aligned} \tag{21}$$

$$\begin{aligned}\rho_{\mathrm{F}22} &= \frac{1}{4}\{2 + w(2-4k) \\ &\quad + p[v-w-1+2kw+t_3(1-2k)]\},\end{aligned} \tag{22}$$

$$\rho_{\mathrm{F}33} = -\frac{1}{4}p[v+w-1-2kw+t_3(2k-1)], \tag{23}$$

$$\rho_{\mathrm{F}44} = -\frac{1}{4}p[v-w-1+2kw+t_3(1-2k)], \tag{24}$$

$$\rho_{\mathrm{F}23} = \rho_{\mathrm{F}32} = \frac{1}{4}\sqrt{p}(t_1 - t_2 + 2kt_2), \tag{25}$$

$$\rho_{\mathrm{F14}} = \rho_{\mathrm{F41}} = \frac{1}{4}\sqrt{p}(t_1 + t_2 - 2kt_2). \tag{26}$$

For Pauli operators σ_1, σ_2, and σ_3, one can use the steering criterion from the entropic uncertainty relation[11]

$$H(\sigma_1^{\mathrm{B}}|\sigma_1^{\mathrm{A}}) + H(\sigma_2^{\mathrm{B}}|\sigma_2^{\mathrm{A}}) + H(\sigma_3^{\mathrm{B}}|\sigma_3^{\mathrm{A}}) \geq 2 \tag{27}$$

to verify the EPR steering from Alice to Bob for arbitrarily two-qubit state ρ. $H(Q|R) = H(\rho_{QR}) - H(\rho_R)$ is the conditional entropy of the bilateral measurements. Here, $\rho_R = \mathrm{Tr}_Q(\rho_{QR})$, $H(\rho) = -\sum_i p_i \log p_i$, and $p_i = \mathrm{Tr}(\rho M_i)$ is the probability of measurement outcome i for the observable M. Violation of the inequality signifies that Bob can be steered by Alice. Specially, for the two-qubit X state of Eq. (19), one can use the violation of the inequality[39,40]

$$\begin{aligned} I^{\mathrm{A}\to\mathrm{B}}(\rho_{\mathrm{AB}}^{\mathrm{X}}) = & \sum_{i=1,2} [(1+t_i)\log(1+t_i) + (1-t_i)\log(1-t_i)] \\ & -(1+v)\log(1+v) - (1-v)\log(1-v) \\ & +\frac{1}{2}\big[(1+t_3+v+w)\log(1+t_3+v+w) \\ & +(1+t_3-v-w)\log(1+t_3-v-w) \\ & +(1-t_3-v+w)\log(1-t_3-v+w) \\ & +(1-t_3+v-w)\log(1-t_3+v-w)\big] \leq 2 \end{aligned} \tag{28}$$

to detect the EPR steering from Alice to Bob. Therefore, for the final state ρ_{F}, we can use

$$S^{\mathrm{A}\to\mathrm{B}} = \max\left\{0, \frac{I^{\mathrm{A}\to\mathrm{B}}(\rho_{\mathrm{F}}) - 2}{I^{\mathrm{A}\to\mathrm{B}}(\rho_{\max}) - 2}\right\} \tag{29}$$

to represent the steerability from Alice to Bob. $I^{\mathrm{A}\to\mathrm{B}}(\rho_{\max}) = 6$[39,40] ($\rho_{\max}$ is the maximally entangled state) is the normalization factor. Based on the ρ_{F}, we can derive

$$\begin{aligned} I^{\mathrm{A}\to\mathrm{B}}(\rho_{\mathrm{F}}) = & \frac{1}{2\log 2}\Big(I_1^{\mathrm{A}\to\mathrm{B}} + I_2^{\mathrm{A}\to\mathrm{B}} + I_3^{\mathrm{A}\to\mathrm{B}} \\ & + I_4^{\mathrm{A}\to\mathrm{B}} + I_5^{\mathrm{A}\to\mathrm{B}}\Big), \end{aligned} \tag{30}$$

$$\begin{aligned} I_1^{\mathrm{A}\to\mathrm{B}} = & 2(1-t_1\sqrt{p})\log(1-t_1\sqrt{p}) \\ & +2(1+t_1\sqrt{p})\log(1+t_1\sqrt{p}) \\ & +2(1-t_2\sqrt{p}+2kt_2\sqrt{p})\log(1-t_2\sqrt{p}+2kt_2\sqrt{p}) \\ & +2(1+t_2\sqrt{p}-2kt_2\sqrt{p})\log(1+t_2\sqrt{p}-2kt_2\sqrt{p}) \\ & -2(2-p+pv)\log(2-p+pv) \\ & -2(p-pv)\log(p-pv), \end{aligned} \tag{31}$$

$$\begin{aligned} I_2^{\mathrm{A}\to\mathrm{B}} = & p[1-t_3+2kt_3-v+w-2kw] \\ & \times\log\{p[1-t_3+2kt_3-v+w-2kw]\}, \end{aligned} \tag{32}$$

$$\begin{aligned} I_3^{\mathrm{A}\to\mathrm{B}} = & p[1+t_3-2kt_3-v-w+2kw] \\ & \times\log\{p[1+t_3-2kt_3-v-w+2kw]\}, \end{aligned} \tag{33}$$

$$\begin{aligned} I_4^{\mathrm{A}\to\mathrm{B}} = & \{2+w(4k-2)+p[-1-t_3+2kt_3+v+w-2kw]\} \\ & \times\log\big\{2+w(4k-2) \\ & +p[-1-t_3+2kt_3+v+w-2kw]\big\}, \end{aligned} \tag{34}$$

$$\begin{aligned} I_5^{\mathrm{A}\to\mathrm{B}} = & \{2+w(2-4k)+p[-1+t_3-2kt_3+v-w+2kw]\} \\ & \times\log\big\{2+w(2-4k) \\ & +p[-1+t_3-2kt_3+v-w+2kw]\big\}. \end{aligned} \tag{35}$$

Similarly, for a two-qubit X state, the violation of the inequality

$$\begin{aligned} I^{\mathrm{B}\to\mathrm{A}}(\rho_{\mathrm{AB}}^{\mathrm{X}}) = & \sum_{i=1,2} [(1+t_i)\log(1+t_i) + (1-t_i)\log(1-t_i)] \\ & -(1+w)\log(1+w) - (1-w)\log(1-w) \\ & +\frac{1}{2}\big[(1+t_3+v+w)\log(1+t_3+v+w) \\ & +(1+t_3-v-w)\log(1+t_3-v-w) \\ & +(1-t_3-v+w)\log(1-t_3-v+w) \\ & +(1-t_3+v-w)\log(1-t_3+v-w)\big] \leq 2 \end{aligned} \tag{36}$$

means that Bob can steer Alice.[39,40] Thus, the steerability from Bob to Alice is

$$S^{\mathrm{B}\to\mathrm{A}} = \max\left\{0, \frac{I^{\mathrm{B}\to\mathrm{A}}(\rho_{\mathrm{F}}) - 2}{I^{\mathrm{B}\to\mathrm{A}}(\rho_{\max}) - 2}\right\}, \tag{37}$$

$$\begin{aligned} I^{\mathrm{B}\to\mathrm{A}}(\rho_{\mathrm{F}}) = & \frac{1}{2\log 2}\big(I_1^{\mathrm{B}\to\mathrm{A}} + I_2^{\mathrm{A}\to\mathrm{B}} + I_3^{\mathrm{A}\to\mathrm{B}} \\ & + I_2^{\mathrm{B}\to\mathrm{A}} + I_5^{\mathrm{A}\to\mathrm{B}}\big), \end{aligned} \tag{38}$$

$$\begin{aligned} I_1^{\mathrm{B}\to\mathrm{A}} = & 2(1-t_1\sqrt{p})\log(1-t_1\sqrt{p}) \\ & +2(1+t_1\sqrt{p})\log(1+t_1\sqrt{p}) \\ & +2(1-t_2\sqrt{p}+2kt_2\sqrt{p})\log(1-t_2\sqrt{p}+2kt_2\sqrt{p}) \\ & +2(1+t_2\sqrt{p}-2kt_2\sqrt{p})\log(1+t_2\sqrt{p}-2kt_2\sqrt{p}) \\ & -2(1+w-2kw)\log(1+w-2kw), \end{aligned} \tag{39}$$

$$\begin{aligned} I_2^{\mathrm{B}\to\mathrm{A}} = & -2(1-w+2kw)\log(1-w+2kw) \\ & +\{2+w(4k-2) \\ & +p[-1-t_3+2kt_3+v+w-2kw]\} \\ & \times\log\{2+w(4k-2) \\ & +p[-1-t_3+2kt_3+v+w-2kw]\}. \end{aligned} \tag{40}$$

The difference between $S^{\mathrm{B}\to\mathrm{A}}$ and $S^{\mathrm{A}\to\mathrm{B}}$ is introduced by

$$S^{\Delta} = S^{\mathrm{B}\to\mathrm{A}} - S^{\mathrm{A}\to\mathrm{B}}, \tag{41}$$

which represents the degree of asymmetry between $S^{\mathrm{B}\to\mathrm{A}}$ and $S^{\mathrm{A}\to\mathrm{B}}$ in different orientations (namely, from Bob to Alice or from Alice to Bob).

4. Revealing the EPR steering and its directions under different values of *t*

To start with, we concentrate on ascertaining the influences of auxiliary qubits on EPR steering and its directions

under different values of t. Figure 1 provides the EPR steering with different t in the strong coupling regime ($\lambda = 2, \gamma_0 = 12$). One can demonstrate from Fig. 1(a) that $S^{A\to B}$ and $S^{B\to A}$ decline with increasing t in the absence of auxiliary atoms ($N = 1$), and finally reach zero at corresponding values of t, respectively. S^{Δ} increases and then decreases as t decreases. Of particular note is that there is a yellow area in the Fig. 1(a) in which $S^{A\to B} = 0$ and $S^{B\to A} \neq 0$ are obeyed. The results reveal that EPR steering from Bob to Alice can be demonstrated via the entropy uncertainty relation in the yellow area, whether Alice can steer Bob is unknown in this area. In the left region of the yellow area of Fig. 1(a) $S^{A\to B} \neq 0$ and $S^{B\to A} \neq 0$, and $S^{A\to B} = S^{B\to A} = 0$ is satisfied in the right region of the yellow area. That is to say, the system can realize the both-way EPR steering (i.e., Alice and Bob can steer each other) if the value of t locates in the left region of the yellow area (namely, small t). The both-way steerability cannot be verified in the right region of the yellow area (i.e., large t), and the region is very large and extends to $t \to \infty$. If one adds two auxiliary qubits ($N = 3$) in Fig. 1(b), $S^{B\to A}$ and S^{Δ} behave as damped oscillations, which are different from those in Fig. 1(a). In addition, the yellow areas in Fig. 1(b) are very wide, implying that Bob can steer Alice in most cases. The system is in the both-way steerable state in the left region of the first yellow area, and both-way EPR steering cannot be confirmed in the narrow area between the two yellow regions in Fig. 1(b). If the auxiliary qubits increase to eight ($N = 9$) in Fig. 1(c), $S^{A\to B}$, $S^{B\to A}$ and S^{Δ} have oscillatory dynamics as t continues to enhance. The yellow region shrinks into two narrow areas, and steerability from Bob to Alice (from Alice to Bob) can (cannot) be demonstrated in the two regions. Remarkably, $S^{A\to B} \neq 0$ and $S^{B\to A} \neq 0$ are obeyed in the very large region of t, except for the two narrow yellow areas in Fig. 1(c). The results indicate that the system can achieve both-way EPR steering in the very large area of t when adding eight auxiliary qubits. If one sets the number of auxiliary qubits to 15 ($N = 16$) in Fig. 1(d), $S^{A\to B} \neq 0$ and $S^{B\to A} \neq 0$ can be observed for different values of t, signifying that the both-way EPR steering of the system can be detected via the entropy uncertainty relation. The increase in auxiliary qubits is responsible for the results that steerability from Alice to Bob or from Bob to Alice can be more effectively revealed, especially for revealing the EPR steering from Alice to Bob.

We change the state parameters $v = 0.6$ and $w = 0.5$ to $v = -0.6$ and $w = -0.5$ in Fig. 2, and the influences of auxiliary qubits on EPR steering and its directions are different from those in Fig. 1. To be clearer, $S^{A\to B}$ and $S^{B\to A}$ in the pink areas obey $S^{A\to B} \neq 0$ and $S^{B\to A} = 0$, meaning that Alice can steer Bob in the pink area; however, the steerability from Bob to Alice is unknown. The results are opposite to those in Fig. 1. In the left (right) area of the pink region of Fig. 2(a), the system is in a both-way steerable state (the EPR steering-unknown state). Compared with Fig. 2(a), although the number of pink areas increases to six if $N = 5$ in Fig. 2(b) the area of the both-way steerable state significantly expands, and more states can be revealed to be both-way steerable. If one adds an auxiliary qubit to the six ($N = 7$) in Fig. 2(c), the pink ranges further shrink, $S^{A\to B} \neq 0$ and $S^{B\to A} \neq 0$ can be observed in the broader region of t. $S^{A\to B} \neq 0$ and $S^{B\to A} \neq 0$ are satisfied for all values of t by setting $N = 11$ in Fig. 2(d), and both-way EPR steering can be more effectively verified by introducing more auxiliary qubits.

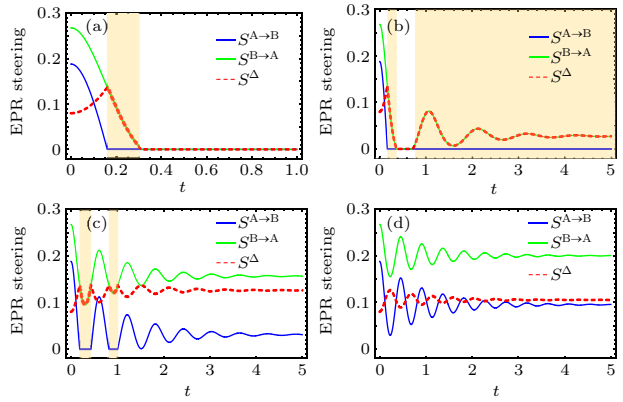


Fig. 1. EPR steering with respect to t when ($\lambda = 2$, $\gamma_0 = 12$): (a) $N = 1$, (b) $N = 3$, (c) $N = 9$, (d) $N = 16$. For all figures, $t_1 = 0.7$, $t_2 = 0.9$, $t_3 = -0.8$, $k = 0.9$, $v = 0.6$ and $w = 0.5$. The $S^{A\to B}$ and $S^{B\to A}$ in the yellow areas obey $S^{A\to B} = 0$ and $S^{B\to A} \neq 0$.

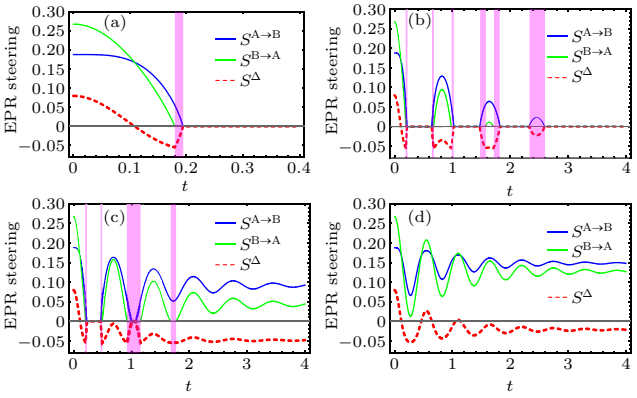


Fig. 2. The EPR steering with respect to t when ($\lambda = 2, \gamma_0 = 12$): (a) $N = 1$, (b) $N = 5$, (c) $N = 7$, (d) $N = 11$. For all figures, $t_1 = 0.7$, $t_2 = 0.9$, $t_3 = -0.8$, $k = 0.9$, $v = -0.6$ and $w = -0.5$. The $S^{A\to B}$ and $S^{B\to A}$ in the pink areas obey $S^{A\to B} \neq 0$ and $S^{B\to A} = 0$.

Now, we investigate the effects of auxiliary qubits on the EPR steering and its directions in the weak coupling regime ($\lambda = 12, \gamma_0 = 2$). As found from Fig. 3(a), an increase in t induces the decrease of $S^{A\to B}$ and $S^{B\to A}$. $S^{A\to B}$ and $S^{B\to A}$ finally disappear. S^{Δ} increases and then decreases with increasing t. One can only reveal the both-way EPR steering when t is small. The results are similar to those for the strong coupling regime in Fig. 1(a). Notably, the yellow areas ($S^{A\to B} = 0$ and $S^{B\to A} \neq 0$) expand to $t \to \infty$ when the number of auxiliary particles reaches 4 ($N = 5$) and 6 ($N = 7$) in Figs. 3(b) and 3(c).

The steerability from Bob to Alice can always be witnessed for different values of t, and the steerability from Alice to Bob can only be captured at small t. Meanwhile, the phenomena of damping oscillations of $S^{A\to B}$ and $S^{B\to A}$ vanish in Figs. 3(b) and 3(c), which are different from those in the strong coupling regime. The auxiliary qubit ($N-1=8$) gives rise to the complete satisfaction of $S^{A\to B}\neq 0$ and $S^{B\to A}\neq 0$ in Fig. 3(d), manifesting that the system can achieve both-way steering.

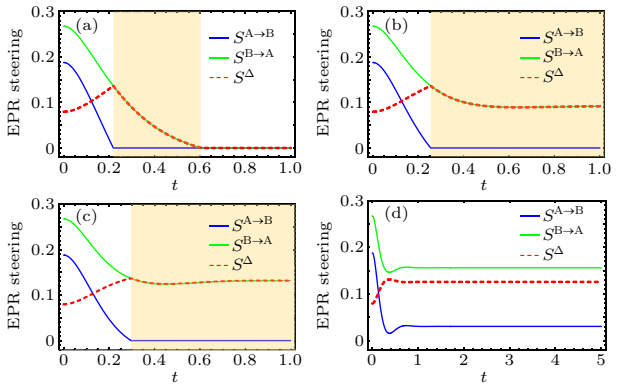


Fig. 3. The EPR steering with respect to t when $(\lambda=12,\gamma_0=2)$: (a) $N=1$, (b) $N=5$, (c) $N=7$, (d) $N=9$. For all figures, $t_1=0.7$, $t_2=0.9$, $t_3=-0.8$, $k=0.9$, $v=0.6$ and $w=0.5$. The $S^{A\to B}$ and $S^{B\to A}$ in the yellow areas obey $S^{A\to B}=0$ and $S^{B\to A}\neq 0$.

In Fig. 4, we set state parameters $v=-0.6$ and $w=-0.5$ for the weak coupling regime. It is revealed from Figs. 4(a)–4(c) that $S^{A\to B}\neq 0$ and $S^{B\to A}=0$ are obeyed in the narrow pink intervals (these results are different from those of $v=0.6$ and $w=0.5$ in Figs. 3(a)–3(c)), in which one can only detect EPR steering from Alice to Bob. The system is in the both-way steerable state when the value of t is on the left of the pink interval. Also, as N increases from 1 to 4, the pink ranges inflate and also move toward the direction of large t. Namely, the tasks where Alice steers Bob or Bob steers Alice can be achieved in the larger range of t by introducing more auxiliary qubits. Finally, Alice and Bob can always steer each other if one adds six ($N=7$) auxiliary qubits in Fig. 4(d).

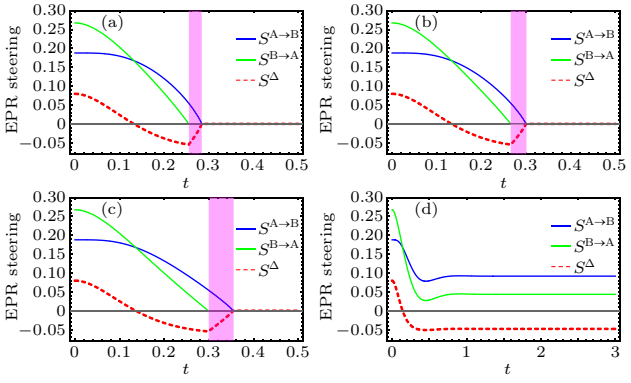


Fig. 4. The EPR steering with respect to t when $(\lambda=12,\gamma_0=2)$: (a) $N=1$, (b) $N=2$, (c) $N=4$, (d) $N=7$. For all figures, $t_1=0.7$, $t_2=0.9$, $t_3=-0.8$, $k=0.9$, $v=-0.6$ and $w=-0.5$. The $S^{A\to B}$ and $S^{B\to A}$ in the pink areas obey $S^{A\to B}\neq 0$ and $S^{B\to A}=0$.

5. Uncovering the EPR steering and its directions with various values of N

In this section, we focus our attention on exploring EPR steering with different values of N. The investigations of Section 3 reveal that the both-way steerability can be realized at small t. Hence, figure 5 characterizes the dependence of the EPR steering on N when considering $t=1$. For the strong coupling regime $(\lambda=2,\gamma_0=12)$ and $(v=0.6,w=0.5)$ in Fig. 5(a), $S^{B\to A}$ rapidly strengthens with N. Subsequently, an increase in N induces the oscillatory enlargement of $S^{B\to A}$. Compared with $S^{B\to A}$, one needs more auxiliary qubits to realize $S^{A\to B}\neq 0$. For this reason, both-way EPR steering can be uncovered with the help of more auxiliary qubits, and only the steerability from Bob to Alice can be demonstrated by using fewer auxiliary qubits (the yellow region appears in the region of small N). The degree of asymmetry (S^{Δ}) between $S^{B\to A}$ and $S^{A\to B}$ first increases and then decreases with the oscillation. If one changes $(v=0.6,w=0.5)$ in Fig. 5(a) into $(v=-0.6,w=-0.5)$ in Fig. 5(b), the characteristics of oscillatory enhancements of $S^{A\to B}$ and $S^{B\to A}$ are invariant. Of particular note is that the directionality of the EPR steering varies in Fig. 5(b). To be clearer, one can only use fewer auxiliary qubits to reveal EPR steering from Alice to Bob (the pink areas appear in the area of small N).

Considering the weak coupling regime $(\lambda=12,\gamma_0=2)$ in Figs. 5(c) and 5(d), the particularities of $S^{A\to B}$, $S^{B\to A}$ and S^{Δ} are different from those of the strong coupling regime in Figs. 5(a) and 5(b). $S^{A\to B}$ and $S^{B\to A}$ monotonously enhance as N increases, and S^{Δ} monotonously increases or decreases in Figs. 5(c) and 5(d). The yellow or pink region locates in the region of small N, and only the EPR steering from Bob to Alice (the EPR steering from Alice to Bob) can be witnessed by employing fewer auxiliary qubits in Fig. 5(c) (Fig. 5(d)). More auxiliary qubits are conducive to revealing the both-way EPR steering of system.

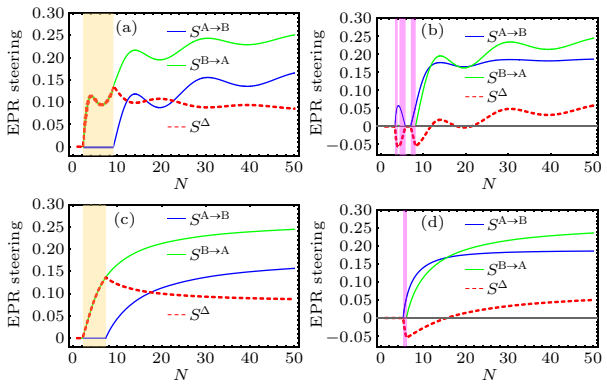


Fig. 5. The EPR steering with respect to N: (a) $\lambda=2$, $\gamma_0=12$, $v=0.6$, $w=0.5$; (b) $\lambda=2$, $\gamma_0=12$, $v=-0.6$, $w=-0.5$; (c) $\lambda=12$, $\gamma_0=2$, $v=0.6$, $w=0.5$; (d) $\lambda=12$, $\gamma_0=2$, $v=-0.6$, $w=-0.5$. For all figures, $t_1=0.7$, $t_2=0.9$, $t_3=-0.8$, $k=0.9$ and $t=1$. The $S^{A\to B}$ and $S^{B\to A}$ in the yellow areas obey $S^{A\to B}=0$ and $S^{B\to A}\neq 0$. The $S^{A\to B}$ and $S^{B\to A}$ in the pink areas obey $S^{A\to B}\neq 0$ and $S^{B\to A}=0$.

6. Disclosing the EPR steering and its directions under different values of k

Here, we use auxiliary qubits to reveal the EPR steering and its directions under different values of k. It is found in Fig. 6 that the yellow regions locate in small or large values of k, in which the EPR steering from Alice to Bob is unknown and the steerability from Bob to Alice is confirmed. In the left of the first yellow area (or in the right of the second yellow area) of Fig. 6(a), $S^{\mathrm{A}\to\mathrm{B}} \neq S^{\mathrm{B}\to\mathrm{A}} \neq 0$ is obeyed, and the system is in the both-way steerable state. In the area between the two yellow regions, $S^{\mathrm{A}\to\mathrm{B}} = S^{\mathrm{B}\to\mathrm{A}} = 0$ is satisfied, and both-way EPR steering is uncertain through the entropy uncertainty relation. As demonstrated from Figs. 6(b)–6(d), the increase in auxiliary qubits ($N-1=5$, 11 and 19) leads to the phenomenon that the yellow areas shrink and move toward the direction of $k=0.5$. As a consequence, the introductions of more auxiliary qubits can help us to reveal more steerable states from Alice to Bob or from Bob to Alice under various values of k. Of particular note is that the steerability near $k=0.5$ cannot be ascertained by coupling more auxiliary qubits.

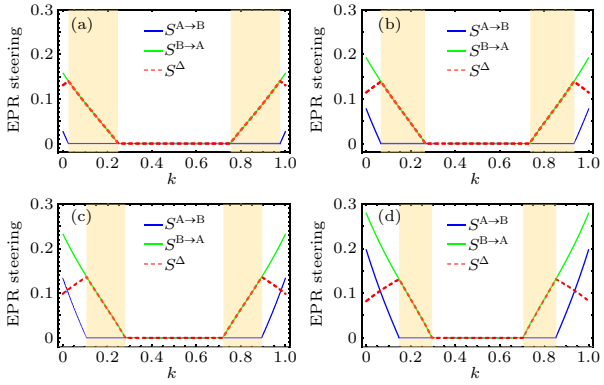


Fig. 6. The EPR steering with respect to k when $(\lambda=2,\gamma_0=12)$: (a) $N=1$, (b) $N=6$, (c) $N=12$, (d) $N=20$. For all figures, $t_1=0.7$, $t_2=0.9$, $t_3=-0.8$, $t=0.2$, $v=0.6$ and $w=0.5$. The $S^{\mathrm{A}\to\mathrm{B}}$ and $S^{\mathrm{B}\to\mathrm{A}}$ in the yellow areas obey $S^{\mathrm{A}\to\mathrm{B}}=0$ and $S^{\mathrm{B}\to\mathrm{A}}\neq 0$.

If one sets $v=-0.6$ and $w=-0.5$ in Fig. 7, the results will reveal characteristics that different from those in Fig. 6. In the two pink areas ($S^{\mathrm{A}\to\mathrm{B}}\neq 0$ and $S^{\mathrm{B}\to\mathrm{A}}=0$) of Fig. 7(a), the steerability from Alice to Bob can be captured through the entropy uncertainty relation; whether Bob can steer Alice is unknown. The results are different from those in Fig. 6(a). Moreover, the pink regions of Fig. 7(a) are significantly narrower than the yellow areas of Fig. 6(a), and the pink regions are further away from $k=0$ and $k=1$. One can more effectively verify that the system is both-way steerable in the cases of $v=-0.6$ and $w=-0.5$ by setting $N=1$ (i.e., the absence of auxiliary atoms). Assuming one increases N from 10 to 40, the pink regions shrink when $N=10$ in Fig. 7(b) and vanish when $N=20$ in Fig. 7(c). It deserves to be emphasized that there are two yellow regions ($S^{\mathrm{A}\to\mathrm{B}}=0$ and $S^{\mathrm{B}\to\mathrm{A}}\neq 0$) in Fig. 7(d) if $N=40$. One can only reveal the EPR steering from Bob to Alice; whether Alice can steer Bob is uncertain. The results are different from those in Figs. 7(a) and 7(b). That is, the increase of auxiliary particles ($N-1=39$) changes the direction of the EPR steering that can be detected under different values of k via the entropy uncertainty relation (i.e., it changes the case that the steerability from Alice to Bob is certain in the pink areas of Figs. 7(a) and 7(b) into the case that the steerability from Bob to Alice is certain in the yellow areas of Fig. 7(d)). These results cannot be revealed in Figs. 1–6.

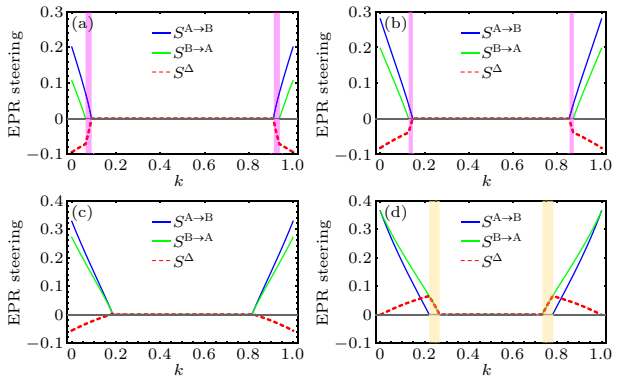


Fig. 7. The EPR steering with respect to k when $(\lambda=2,\gamma_0=12)$: (a) $N=1$, (b) $N=10$, (c) $N=20$, (d) $N=40$. For all figures, $t_1=0.7$, $t_2=0.9$, $t_3=-0.8$, $t=0.2$, $v=-0.6$ and $w=-0.5$. The $S^{\mathrm{A}\to\mathrm{B}}$ and $S^{\mathrm{B}\to\mathrm{A}}$ in the yellow areas obey $S^{\mathrm{A}\to\mathrm{B}}=0$ and $S^{\mathrm{B}\to\mathrm{A}}\neq 0$. The $S^{\mathrm{A}\to\mathrm{B}}$ and $S^{\mathrm{B}\to\mathrm{A}}$ in the pink areas obey $S^{\mathrm{A}\to\mathrm{B}}\neq 0$ and $S^{\mathrm{B}\to\mathrm{A}}=0$.

Now, our attention is confined to exploring the EPR steering with different values of k for the weak coupling regime $(\lambda=12,\gamma_0=2)$ in Figs. 8 and 9. By comparing Fig. 8(a) (or Figs. 8(b)–8(d)) with Fig. 6(a) (or Figs. 6(b)–6(d)), one can conclude that the results in the weak coupling regime are similar to those in the strong coupling regime. The difference between Fig. 8(a) (or Figs. 8(b)–8(d)) and Fig. 6(a) (or Figs. 6(b)–6(d)) is that the yellow areas are narrower and closer to $k=0.5$ in Fig. 8(a) (or Figs. 8(b)–8(d)). The results imply that one can capture more steerable states in the weak coupling regime by coupling auxiliary particles.

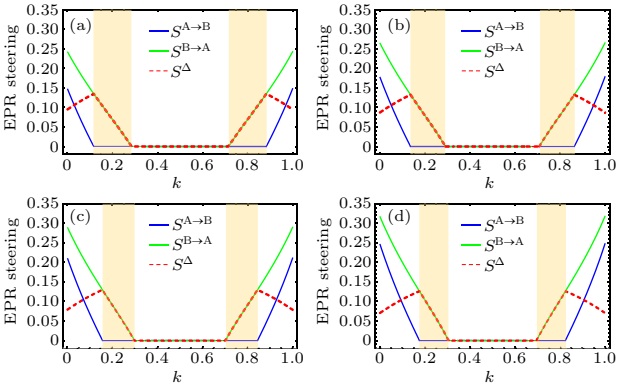


Fig. 8. The EPR steering with respect to k when $(\lambda=12,\gamma_0=2)$: (a) $N=1$, (b) $N=6$, (c) $N=12$, (d) $N=20$. For all figures, $t_1=0.7$, $t_2=0.9$, $t_3=-0.8$, $t=0.2$, $v=0.6$ and $w=0.5$. The $S^{\mathrm{A}\to\mathrm{B}}$ and $S^{\mathrm{B}\to\mathrm{A}}$ in the yellow areas obey $S^{\mathrm{A}\to\mathrm{B}}=0$ and $S^{\mathrm{B}\to\mathrm{A}}\neq 0$.

In the final stage, figure 9 provides the dependence of EPR steering on k for $(v=-0.6, w=-0.5)$ in the weak coupling regime $(\lambda=12, \gamma_0=2)$. The two pink areas are very narrow in Fig. 9(a), and EPR steering from Alice to Bob (from Bob to Alice) is certain (uncertain) in these regions. Meanwhile, the ranges of the both-way steerable states (on the left of the first pink area or on the right of the second pink area) in Fig. 9(a) are more expansive than the corresponding ranges in Fig. 7(a). By introducing more auxiliary particles, the pink regions disappear if $N=7$ in Fig. 9(b), and the yellow regions appear if $N=18$ and $N=30$ in Figs. 9(c) and 9(d). In other words, the introductions of more auxiliary particles changes the situation that steerability from Alice to Bob is certain in the pink areas of Fig. 9(a) into a situation where the steerability from Bob to Alice is certain in the yellow areas of Figs. 9(c) and 9(d). Moreover, compared with the pink areas of Fig. 9(a), the yellow areas of Figs. 9(c) and 9(d) are further far away from $k=0$ and $k=1$. That is, more both-way steerable states are revealed by adding more auxiliary particles.

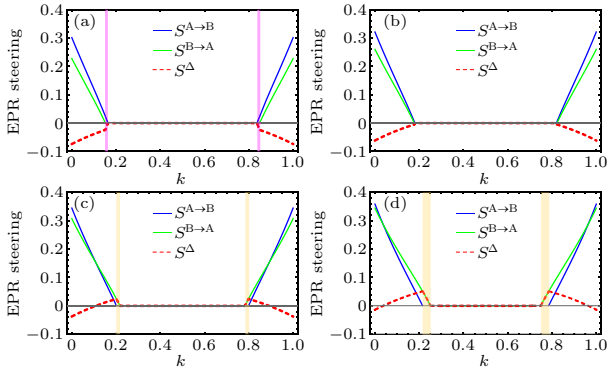


Fig. 9. The EPR steering with respect to k when $(\lambda=12, \gamma_0=2)$: (a) $N=1$, (b) $N=7$, (c) $N=18$, (d) $N=30$. For all figures, $t_1=0.7$, $t_2=0.9$, $t_3=-0.8$, $t=0.2$, $v=-0.6$ and $w=-0.5$. The $S^{A\to B}$ and $S^{B\to A}$ in the yellow areas obey $S^{A\to B}=0$ and $S^{B\to A}\neq 0$. The $S^{A\to B}$ and $S^{B\to A}$ in the pink areas obey $S^{A\to B}\neq 0$ and $S^{B\to A}=0$.

7. Conclusions

Assuming Alice and Bob share a two-qubit X state, and the two-qubit X state is composed of two atoms. The atom of Alice suffers from the reservoir and the atom of Bob couples with the bit flip channel. We reveal how the auxiliary qubits influence the EPR steering and its directions by means of the entropy uncertainty relation. The results indicate that $S^{A\to B}$ and $S^{B\to A}$ quickly decrease (behave as damped oscillations) as t goes if one introduces fewer auxiliary qubits (more auxiliary qubits) in the strong coupling regime. Considering state parameters $(v=0.6, w=0.5)$, there are many yellow areas in which $S^{A\to B}=0$ and $S^{B\to A}\neq 0$ are satisfied. The steerability from Bob to Alice can be revealed via the entropy uncertainty relation; whether Alice can steer Bob is uncertain. If $(v=-0.6, w=-0.5)$, $S^{A\to B}\neq 0$ and $S^{B\to A}=0$ are obeyed in the pink ranges, and one can only verify the EPR steering from Alice to Bob in these ranges. The yellow areas and pink areas can be eliminated by coupling more auxiliary qubits, and the tasks that Alice steers Bob or Bob steers Alice can be more effectively achieved by adding more auxiliary qubits. In the strong coupling regime, the increase in auxiliary qubits is responsible for the enhancements of $S^{A\to B}$ and $S^{B\to A}$ with the characteristic of oscillation. By contrast, the $S^{A\to B}$ and $S^{B\to A}$ monotonously increase with increasing N in the weak coupling regime. In the strong coupling regime or weak coupling regime, both-way steerability cannot be verified by coupling more auxiliary qubits if the value of the channel parameter k is in the vicinity of 0.5. The yellow regions or pink regions appear near $k=0$ and $k=1$, and these areas shrink and move toward the direction of $k=0.5$ as N increases. That is, the introductions of more auxiliary qubits can be used to reveal the EPR steering in a wider interval of k. The system is in the both-way steerable state ($S^{A\to B}\neq 0$ and $S^{B\to A}\neq 0$ are satisfied) if the values of k locate in the left intervals of the first yellow or pink areas (or in the right intervals of the second yellow or pink areas). Of particular note is that increases in N can change the scenario that the steerability from Alice to Bob is certain in the pink intervals into the scenario that the steerability from Bob to Alice is certain in the yellow intervals if $(v=-0.6, w=-0.5)$.

Acknowledgments

Project supported by the National Natural Science Foundation of China (Grant No. 12175001), the Key Project of Natural Science Research of West Anhui University (Grant No. WXZR202311), the Natural Science Research Key Project of Education Department of Anhui Province of China (Grant Nos. KJ2021A0943, 2022AH051681, and 2023AH052648), the Open Fund of Anhui Undergrowth Crop Intelligent Equipment Engineering Research Center (Grant No. AUCIEERC-2022-01), Anhui Undergrowth Crop Intelligent Equipment Engineering Research Center (Grant No. 2022AH010091), the University Synergy Innovation Program of Anhui Province (Grant No. GXXT-2021-026), the Anhui Provincial Natural Science Foundation (Grant Nos. 2108085MA18 and 2008085MA20), Key Project of Program for Excellent Young Talents of Anhui Universities (Grant No. gxyqZD2019042), the open project of the Key Laboratory of Functional Materials and Devices for Informatics of Anhui Higher Education Institutes (Grant No. FMDI202106), and the research start-up funding project of High Level Talent of West Anhui University (Grant No. WGKQ2021048).

References

[1] Einstein A, Podolsky B and Rosen N 1935 *Phys. Rev.* **47** 777
[2] Schrödinger E 1935 *Math. Proc. Cambridge Philos. Soc.* **31** 555

[3] Uola R, Costa A C S, Nguyen H C and Guhne O 2020 *Rev. Mod. Phys.* **92** 015001
[4] Wiseman H M, Jones S J and Doherty A C 2007 *Phys. Rev. Lett.* **98** 140402
[5] Zhen Y Z, Zheng Y L, Cao W F, Li L, Chen Z B, Liu N L and Chen K 2016 *Phys. Rev. A* **93** 012108
[6] Cavalcanti E G, Jones S J, Wiseman H M and Reid M D 2009 *Phys. Rev. A* **80** 032112
[7] Costa A C S and Angelo R M 2016 *Phys. Rev. A* **93** 020103
[8] Zukowski M, Dutta A and Yin Z 2015 *Phys. Rev. A* **91** 032107
[9] Li J, Wang C Y, Liu T J and Wang Q 2018 *Phys. Rev. A* **97** 032107
[10] Walborn S P, Salles A, Gomes R M, Toscano F and Souto Ribeiro P H 2011 *Phys. Rev. Lett.* **106** 130402
[11] Schneeloch J, Broadbent C J, Walborn S P, Cavalcanti E G and Howell J C 2013 *Phys. Rev. A* **87** 062103
[12] Costa A C S, Uola R and Gühne O 2018 *Phys. Rev. A* **98** 050104
[13] Kriváchy T, Fröwis F and Brunner N 2018 *Phys. Rev. A* **98** 062111
[14] Wollmann S, Uola R and Costa A C S 2020 *Phys. Rev. Lett.* **125** 020404
[15] Zhao F, Yang H, Song X K, Wang D and Ye L 2021 *Phys. Rev. A* **104** 052425
[16] Yang H, Ding Z Y, Wang D, Yuan H, Song X K, Yang J, Zhang C J and Ye L 2020 *Phys. Rev. A* **101** 022324
[17] Wang Y, Hao Z Y, Li J K, Liu Z H, Sun K, Xu J S, Li C F and Guo G C 2023 *Phys. Rev. Lett.* **130** 200202
[18] Guo J, Sun F X, Zhu D, Gessner M, He Q and Fadel M 2023 *Phys. Rev. A* **108** 012435
[19] Liu Y, Cai Y, Luo B, Yan Y, Niu M, Li F and Zhang Y 2021 *Phys. Rev. A* **104** 033704
[20] Ming F, Song X K, Ling J, Ye L and Wang D 2020 *Eur. Phys. J. C* **80** 275
[21] Yang H, Xing L L, Ding Z Y, Zhang G and Ye L 2022 *Chin. Phys. B* **31** 090302
[22] Liu S, Han D, Wang N, Xiang Y, Sun F, Wang M, Qin Z, Gong Q, Su X and He Q 2023 *Phys. Rev. Lett.* **128** 200401
[23] Zhu J, Hu M J, Li C F, Guo G C and Zhang Y S 2022 *Phys. Rev. A* **105** 032211
[24] Wang M, Xiang Y, Kang H, Han D, Liu Y, He Q, Gong Q, Su X and Peng K 2020 *Phys. Rev. Lett.* **125** 260506
[25] Cai Y, Xiang Y, Liu Y, He Q and Treps N 2020 *Phys. Rev. Res.* **2** 032046
[26] Yang H, Ding Z Y, Wang D, Yuan H, Song X K, Yang J, Zhang C J and Ye L 2020 *Phys. Rev. A* **101** 042115
[27] Yang H, Zhao F, Fan X G, Ding Z Y, Wang D, Song X K, Yuan H, Zhang C J and Ye L 2021 *Opt. Express* **29** 26822
[28] Yang H, Ding Z Y, Song X K, Yuan H, Wang D, Yang J, Zhang C J and Ye L 2021 *Phys. Rev. A* **103** 022207
[29] Xiao Y, Ye X J, Sun K, Xu J S, Li C F and Guo G C 2017 *Phys. Rev. Lett.* **118** 140404
[30] Zheng Z, Yao M, Tong J, Lin Q and Cai Y 2023 *Phys. Rev. A* **108** 012430
[31] Zhang M, Long Y, Zhao S and Zhang X 2022 *Phys. Rev. A* **105** 042435
[32] Zeng Q 2022 *Phys. Rev. A* **106** 032202
[33] Liao C G, Xie H, Chen R X, Ye M Y and Lin X M 2020 *Phys. Rev. A* **101** 032120
[34] Yang Z B, Liu X D, Yin X Y, Ming Y, Liu H Y and Yang R C 2021 *Phys. Rev. Appl.* **15** 024042
[35] Huang X, Zeuthen E, Gong Q and He Q 2019 *Phys. Rev. A* **100** 012318
[36] Maleki Y and Ahansaz B 2020 *Phys. Rev. A* **102** 020402
[37] Xu X X and Hu M L 2022 *Ann. Phys. (Berlin)* **534** 2100412
[38] Nielsen M A and Chuang I L 2000 *Quantum Computation and Quantum Information* (Cambridge: Cambridge University Press)
[39] Sun W Y, Wang D and Ye L 2017 *Laser Phys. Lett.* **14** 095205
[40] Wu S M and Zeng H S 2022 *Eur. Phys. J. C* **82** 716